Evaluation of Novel Liner Concepts for Fan and Airframe Noise Reduction

M. G. Jones*and B. M. Howerton†
NASA Langley Research Center, Hampton, VA 23681

This paper presents a review of four novel liner concepts: soft vanes, over-the-rotor liners, external liners, and flap side-edge liners. A number of similarities in the design and evaluation of these concepts emerged during these investigations. Since these were the first attempts to study these particular liner concepts, there was limited information to guide the design process. In all cases, the target frequencies (or frequency range) were known, but the optimum acoustic impedance and optimum liner placement were typically not known. For these cases, the maximum available surface was used and a ρc-impedance was targeted based on the assumption the sound field impinges on the surface at normal incidence. This choice proved fruitful for every application. An impedance prediction model was used to design variable-depth liner configurations, and a graphical design code (ILIAD) was developed to aid in this process. The ability to build increasingly complex liner configurations via additive manufacturing was key, such that multiple designs could quickly be tested in a normal incidence impedance tube. The Two-Thickness Method was used to evaluate available bulk materials, such that bulk liners could also be considered for each application. These novel liner concepts provide sufficient noise reduction to warrant further investigations.

I. Introduction

A number of novel liner concepts have been explored by the NASA Langley Liner Physics Team over the last decade. These include liner concepts designed for reduction of both aircraft engine fan noise and airframe noise, two significantly different noise generation mechanisms. Each of these liner concepts provides acoustic absorption by inducing viscous dissipation at internal solid structure surfaces (chamber walls for resonant structures, structural ligaments for foam). Many, if not all, also provide pressure-release surfaces (reducing the magnitude of local pressure gradients) in the near-field of the noise generation process, thereby reducing radiation efficiency. This paper explores four novel concepts, and discusses key similarities and differences in their design and implementation.

The first of these concepts is the soft vane,[1,2] wherein a portion of the engine fan exit guide vane surface is made porous to allow communication between pressure fluctuations at the vane surface and multiple, internal, resonant chambers. Soft vanes are intended to reduce rotor-stator interaction noise radiated through the inlet and aft-fan duct. The internal chambers and porous surface are designed to an optimum impedance that minimizes the self-noise generated at the surface of the vane while maximizing absorption of radiated fan noise.

The second concept is an over-the-rotor (OTR) liner, i.e., a liner that is embedded in the nacelle wall at or near the fan rotor plane. OTR liners are also designed to reduce rotor-stator noise. The harsh aeroacoustic environment has prevented conventional liner installation at this location. Also, this portion of the nacelle wall includes a fan containment case intended to contain a broken fan blade. Two distinct types of configurations have been considered for use as OTR liners. The first employs metallic foam,[3,4] which possesses characteristics that support installation in the fan containment case. These characteristics include: (1) containment properties, such that the foam can aid in the blade capture process, (2) low flammability,

*Senior Research Scientist, Research and Technology Directorate, Structural Acoustics Branch, AIAA Associate Fellow.
†Senior Research Scientist, Research and Technology Directorate, Structural Acoustics Branch. AIAA Senior Member.

and (3) minimal fluid retention. With appropriate selection of the metal foam properties, these liners can achieve a selected impedance at the liner surface. Also, since these liners are in the near-field of the tip noise generated by the rotor blades, they provide mitigation of the noise source via a pressure-release surface as well as noise absorption. The second configuration employs multiple, variable-depth, resonant chambers to achieve the desired surface impedance. This concept targets the noise reduction requirements, but is not designed to provide the other features (e.g., containment properties) of metallic foams.

The third liner concept for fan noise reduction is the external liner. This refers to acoustic liners placed on the exterior of the aircraft, e.g., the outer surface of the fuselage. One implementation of these liners is to place liners on the wing or fuselage to reduce fan noise radiated from aircraft engine nacelles (whether from the inlet or the aft bypass duct) that impinges on these airframe components. Alternatively, if an open rotor propulsion system is implemented, there are significant noise concerns due to the lack of a conventional, acoustically treated nacelle for shielding and absorption of rotor noise. In this case, liners integrated into the external surface of the aircraft offer one option for reduction of fan noise radiated to the airport community. There are multiple locations on the aircraft surface that might be suitable for liners, but these will all be combined as a single concept for the purposes of this paper. It should be noted that, due to the location of these liners, it is possible that they would also have some impact on the airframe noise over these surfaces (either absorption of radiated airframe noise or reduction of the airframe noise source mechanism via pressure release). It is also possible that, due to the surface roughness of the liner, they could introduce additional noise (self-noise) and skin friction drag. These topics are left for future studies.

The last concept is a flap side-edge liner that targets airframe noise. A vortex is formed at or near the corner of the flap, and generates noise as it rolls over the surface of the flap. A liner embedded in the edge of the flap presents a lower impedance (relative to hardwall) that inhibits this vortex generation process, and thereby reduces the amount of sound that is generated. Also, the liner is designed (tuned) to absorb sound over the frequency range associated with this noise generation mechanism.

Although these liner concepts are designed for a variety of applications, there are a number of similarities in their respective design approaches. Each concept was designed from the point of view that in order for the liner to provide maximum noise reduction, it would need to present an optimum impedance spectrum at its surface tuned to the specific noise spectrum of interest. For the initial tests, there was typically very limited information regarding the optimum impedance spectra for each application. For those cases where there was no theoretical guidance to determine the optimum surface impedance spectrum, the default choice was to design the liner to achieve a normalized surface impedance of unity (all impedances in this paper are normalized relative to ρc, where ρ and c are the density and sound speed, respectively, for air). Depending on the application, either bulk materials (e.g., metallic foam) and/or single layer, variable depth, perforate-over-honeycomb configurations (resonant structures) were considered as a means to achieve this target surface impedance.

The purpose of this paper is to review these novel liner concepts, as well as the measurement and prediction tools used in their evaluation. Results from tests of each of these concepts are presented, and areas of potential improvements are reviewed. Section II provides a description of some of the tools used in the liner design and evaluation process. Section III provides details regarding the application of these tools for each concept, along with some of the key results. Finally, some of the more interesting results are presented in Section IV.

II. Liner Design and Evaluation

Similar methods were employed to design each of the concepts considered in this study. The common goal was to create a liner that would present a desired acoustic boundary condition at its surface. This boundary condition is the acoustic impedance for local-reacting liner concepts, and is represented as bulk material acoustic properties (e.g., characteristic impedance and propagation constant) for extended-reacting liner concepts. Each local-reacting liner (soft vane, external liner, flap side-edge liner) consists of multiple, variable-depth, resonant chambers covered by a porous facesheet, and each extended-reacting liner (OTR liner, flap side-edge liner) consists of bulk material covered by a porous facesheet.

The design process varied based on the application being considered. For local-reacting liners, an impedance prediction model[5–7] was used to determine the respective depths of the resonant chambers, and to combine these chambers with a porous facesheet to achieve the desired surface impedance spectrum.

There was often insufficient volume to allow for these chambers to be straight and/or perpendicular to the surface of the liner. The Interactive Liner Impedance Analysis and Design (ILIAD) code[8,9] was used to address this concern. ILIAD is a graphical tool that allows the chamber geometry to be drawn in the liner volume while surface impedance and absorption coefficient calculations are updated in real-time based on the impedance prediction model described below. If needed, these chambers can be bent, skewed, or splayed to fit within the available volume.

A simplifying assumption was applied for the extended-reacting liner concepts. Namely, the bulk material that forms the core of the liner was assumed to behave as if it was local reacting. Clearly, this assumption is flawed if one wishes to capture the fine detail of the aeroacoustic environment near the liner surface. However, if the bulk material is a very good absorber of the incident sound, the amount of sound that exits the liner surface at a different location (the dominant feature of an extended-reaction liner) is limited, as that sound has to travel through a greater 'length' of absorbent material to get back to the surface. Thus, if the bulk material properties are chosen to achieve significant absorption, this assumption of local reaction is deemed acceptable for the purposes of this study.

The following provides a brief description of the key tools used in this study. These include the impedance prediction model, the NASA Langley Normal Incidence Tube, and the Two-Thickness Method (TTM). Discussion of the ILIAD code is provided in Section III as it is applied to the soft vane design process.

A. Impedance Prediction Model

Figure 1 provides a sketch of a single chamber of a liner with an interior air gap with height h_1 and a perforate facesheet with thickness h_2. (The thickness of the perforate sheet is exaggerated to demonstrate distinct features of the model used in this study). This model treats each unique portion of the liner chamber separately. In the ensuing discussion, these unique portions (confined to air gaps and perforated sheets in this example) are treated as individual "computational layers."

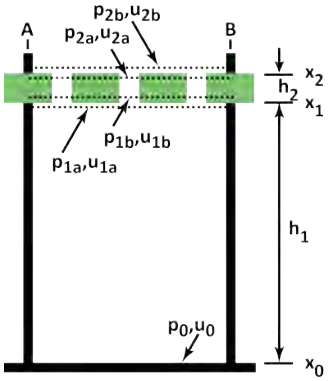

Figure 1: Sketch of single chamber of a liner with key parameters for impedance prediction model.

For the liner concepts considered in this study, each chamber was assumed to be terminated with a rigid, impervious plate. This is incorporated in the model by setting the acoustic pressure, p_0, and particle velocity, u_0, at the backplate to unity and zero, respectively, i.e.,

$$\begin{pmatrix} p_0 \\ u_0 \end{pmatrix} = \begin{pmatrix} 1 \\ 0 \end{pmatrix} \tag{1}$$

This yields an infinite impedance (or zero admittance) at this location. (Acoustic pressures and particle velocities are normalized by ρc^2 and c, respectively.) Changes in the acoustic pressure and particle velocity across the computational layer are computed via

$$\begin{pmatrix} p_{n+1} \\ u_{n+1} \end{pmatrix} = \begin{pmatrix} T_{11} & T_{12} \\ T_{21} & T_{22} \end{pmatrix} \begin{pmatrix} p_n \\ u_n \end{pmatrix} \tag{2}$$

where the transmission coefficients (T_{11}, T_{12}, T_{21} and T_{22}) depend on the modeling approach and the type of layer being considered.

For an open layer (air gap) such as is employed here, the transmission coefficients are given by

$$T_{11} = T_{22} = cosh(k\Gamma h);\ T_{12} = \zeta_c sinh(k\Gamma h);\ T_{21} = \zeta_c^{-1} sinh(k\Gamma h) \tag{3}$$

where $k = \omega/c$ is the free-space wavenumber, ω is the angular frequency, and h is the layer thickness. The propagation constant, Γ, and characteristic impedance, ζ_c, are computed as

$$\Gamma = \sqrt{\frac{J_0(i^{3/2}s)}{J_2(i^{3/2}s)}}\sqrt{\frac{\gamma}{n_\Gamma}}; \qquad \zeta_c = \frac{-i}{\Gamma}\frac{J_0(i^{3/2}s)}{J_2(i^{3/2}s)} \tag{4}$$

where

$$n_\Gamma = \left[1 + \frac{\gamma - 1}{\gamma}\frac{J_0(i^{3/2}\sigma s)}{J_0(i^{3/2}\sigma s)}\right]^{-1} \tag{5}$$

$i = \sqrt{-1}$ is the imaginary unit, $s = (d_c/2)\sqrt{\rho_s\omega/\mu}$ is the shear wave number, and d_c, ρ_s, ω, μ, σ^2 and γ are the channel diameter, static density, angular frequency, coefficient of viscosity, Prandtl number and specific heat ratio, respectively.

Two approaches are considered for computing the change in impedance across perforated sheets. The first assumes the perforated sheet to be a purely resistive lumped element that is too thin to support wave propagation. For this approach, the transmission coefficients for Eq. 2 are given by

$$T_{11} = T_{22} = 1;\ T_{12} = \frac{R_f}{\rho c};\ T_{21} = 0 \tag{6}$$

where the normalized DC flow resistance, $R_f/\rho c$, across the perforated sheet is often estimated from a semi-empirical model (*e.g.*, the Two-Parameter Impedance Prediction Model[10]). The second approach assumes the perforated sheet to be sufficiently thick to support wave propagation. Figure 1 is particularly useful to describe this approach. It is assumed that Eqs. 2 and 3 have been used to determine the acoustic pressure and particle velocity (p_{1a} and u_{1a}) at the top of the air gap. The total acoustic pressure and acoustic mass flow are assumed to be constant across the abrupt area change at the $\{1a,\ 1b\}$ interface, such that

$$p_{1b} = p_{1a}; \qquad NS_{1b}u_{1b} = S_{1a}u_{1a} \tag{7}$$

where N is the number of orifices (3 in this example) connected to a single air cavity, S_{1a} is the cross-sectional area at the top of the air cavity (denoted by the long dashed line at the top of the cavity) and S_{1b} is the cross-sectional area within a single perforate orifice. Next, the wave propagation within the single orifice is computed using Eqs. 2 and 3, where the orifice diameter is used as the 'channel diameter.' Again, the acoustic pressure and acoustic mass flow are assumed to be constant across the $\{2a,\ 2b\}$ interface, such that

$$p_{2b} = p_{2a}; \qquad S_{2b}u_{2b} = NS_{2a}u_{2a} \tag{8}$$

The acoustic pressure and particle velocity at the surface of the chamber (denoted by the dashed line with endpoints A and B) are then used to compute the normalized surface impedance for the chamber via

$$\zeta_{ch} = \frac{p_{2b}}{u_{2b}} \tag{9}$$

This process is repeated for each chamber used to construct the liner. The surface impedance spectra of the individual chambers are then combined to compute the effective impedance across the liner surface. For this computation, it is preferable to use acoustic admittance ($\beta_{ch} = 1/\zeta_{ch}$). The effective admittance across a selected extent of liner surface is given by

$$\beta_s = \Omega \sum_{i=1}^{N_{ch}} \beta_{ch} \tag{10}$$

where N_{ch} represents the number of chambers that combine to form the liner and Ω is the surface open area ratio (porosity) of the liner. The uniform, effective, surface impedance of the liner is then given by $\zeta_s = 1/\beta_s$.

B. Normal Incidence Tube (NIT)

The NIT is a 2 in× 2 in waveguide (Fig. 2) that employs six 120-W compression drivers to generate a plane-wave sound field. This sound field impinges on the surface of the liner and combines with reflections from the liner to create a standing wave pattern. The Two-Microphone Method (TMM)[11,12] is used to measure the complex acoustic pressures at two prescribed distances from the liner surface, such that the frequency dependence of the acoustic impedance of the liner can be computed.

The TMM can be applied with two acoustic source types: discrete frequency tones and random noise. For the discrete frequency tone source, data are acquired for one source frequency at a time, typically for source frequencies from 400 to 3000 Hz in increments of 200 Hz. At each test frequency, reference sound pressure levels (SPL at the reference microphone; see Fig. 2) of 120 and 140 dB are tested such that any liner nonlinearity (sensitivity to acoustic particle velocity and, hence, to source SPL) can be determined. For the random noise source, the overall sound pressure level (OASPL, integrated over frequency range of 400 to 3000 Hz) is typically set to 120 or 140 dB, and data are acquired at frequencies from 400 to 3000 Hz in 25 Hz increments.

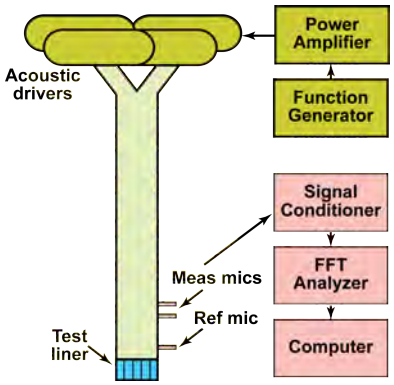

Figure 2: Sketch of NASA Normal Incidence Tube (NIT).

C. Two-Thickness Method

The Two-Thickness Method (TTM)[13] is well established for educing the bulk properties (characteristic impedance, ζ_c, and propagation constant, Γ) for homogeneous absorbing structures that can be regarded as a continuum from the standpoint of acoustic wave propagation. The core of the TTM is the solution of the following two equations:

$$\zeta_1 = \zeta_c \coth(\Gamma T_1); \qquad \zeta_2 = \zeta_c \coth(\Gamma T_2) \tag{11}$$

where ζ_1 and ζ_2 represent measured surface impedances on two separate test samples of thicknesses T_1 and T_2, taken from what is assumed to be a homogeneous, continuous structure. From these two measurements, ζ_c and Γ can be determined as follows:

$$\zeta_c = \sqrt{\zeta_1(2\zeta_2 - \zeta_1)}; \qquad \Gamma = \frac{1}{2d_1} \log \frac{1+a}{1-a} \tag{12}$$

where

$$a = \sqrt{\frac{2\zeta_2 - \zeta_1}{\zeta_1}} \tag{13}$$

The impedance ζ_s of a third sample with thickness T_s can then be predicted using

$$\zeta_s = \zeta_c \coth(\Gamma T_s) \tag{14}$$

A comparison between the measured impedance of the third sample and the impedance predicted using Equation (14) can be used to assess the validity of the educed parameters.

III. Novel Liner Concepts

Soft vanes and over-the-rotor liners[2–4,14] were evaluated in the NASA Glenn Advanced Noise Control Fan (ANCF) and 9- by 15-Foot Low Speed Wind Tunnel (LSWT). External liners were evaluated in the Boeing Low Speed Aeroacoustic Facility (LSAF) as part of a NASA/Boeing collaboration. Flap side-edge liners were evaluated as part of a NASA/Gulfstream collaboration in the NASA Langley 14- by 22-Foot Wind Tunnel. These concepts are discussed in some detail below.

Each of these four concepts is assumed to have two distinct effects on the sound field. First, they provide a surface acoustic impedance to absorb sound that impinges on that surface. Second, since each of these liners is intended to be placed at or near the respective source locations, they are expected to provide a pressure-release surface that inhibits the mechanisms whereby the sound is generated. For now, it is assumed that the same impedance boundary condition (surface impedance) is optimum for both sound absorption and source mitigation.

A. Soft Vane

1. Review

Initial tests of the soft vane concept[1,2,14] were conducted in the NIT and ANCF. There was very limited knowledge regarding the optimum impedance to be applied at the surface of the vane, but previous measurements had indicated that pressure fluctuations impinge on the vane surface at normal incidence (i.e., perpendicular to the surface). The optimum normalized acoustic impedance for sound impinging on a surface at normal incidence is unity, i.e., the characteristic impedance for air (assumed to be at Mach 0.0, since the flow must be brought to a rest at normal incidence). This impedance was selected as the target for the initial design.

The general design approach was to use variable-depth chambers to achieve the desired surface impedance. Given the limited volume, only a limited number of chambers could be incorporated into the design, and those chambers had to be skewed and splayed. There was no clear guidance as to where this treatment should be positioned on the vane surface, i.e., which portion of the vane surface should be made porous and connected to internal chambers.

Thus, the porous surface was positioned to cover from approximately 20% to 60% of the chord length, as this allowed the remainder (forward 20% and aft 40%) of the vane to be used as available volume into which to extend the internal chambers. The porous surface was placed on the suction side of the vane for this initial test.

Multiple configurations were fabricated using additive manufacturing, such that NIT test results could be used to down-select to a final design for use in the ANCF test. Since this occurred at a time when additive manufacturing was in its infancy, the internal chambers were constrained to be full-width slotted chambers (see Fig. 3), presenting yet another issue. Since partitions between adjacent chambers were relatively far apart (manufacturing constraints), internal resistance achieved by scrubbing losses within each chamber was limited. This meant the chambers needed to be filled with a bulk material (i.e., with ceramic beads as depicted in Fig. 3) or covered with a wire mesh to increase the resistance (real component of impedance) at the liner surface. The latter choice (200 MKS Rayls wire mesh facesheet) was chosen as it provided the best results in NIT tests. This configuration was tested in the ANCF, with encouraging results[2] (nominally 1 dB attenuation across 2.5 octaves).

Figure 3: Photograph of soft vane mounted in NIT test fixture.

Follow-on tests were conducted with two 22" fan rigs in the LSWT.[2,14] The first was conducted with the Advanced Ducted Propulsor (ADP) fan. This fan rig produces dominant tones at six frequencies from 1645 to 5306 Hz, corresponding to BPF (blade-passage-frequency) and 2BPF (two times BPF) at the three certification points (takeoff, cutback, and approach). The goal was to simultaneously achieve a ρc impedance (normalized impedance of unity) at each of these frequencies, and to maximize absorption at off-target frequencies. After a number of NIT tests to optimize individual components (e.g., proper combination of number of chambers, chamber depths, and facesheet geometry), a four-chamber configuration (see Fig. 4) was selected. Two key features are noted for this soft vane configuration. First, the interior volume of the vane contains four resonant chambers (the one nearest the leading edge is hard to discern in the photograph) of different lengths and shapes. Second, each of these internal chambers is terminated at the suction surface of the vane, and communicates with the exterior of the vane via a perforated sheet. A wire mesh cover sheet was placed over the perforated sheet in the final assembly, to achieve the desired surface resistance and to present a smooth surface to the mean flow. This soft vane configuration provided 1 to 2 dB noise reduction over at least two octaves.

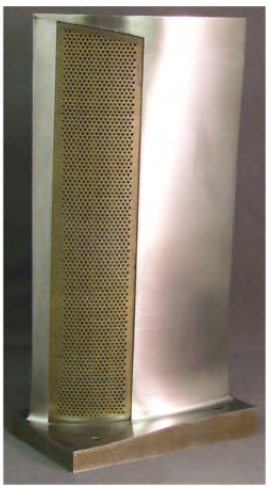

(a) Frontal view.

(b) Side view.

Figure 4: Photographs of soft vane.

The second LSWT test used the Source Diagnostic Test Fan (SDT). A number of lessons learned from the earlier tests were applied in preparation for this test. First, 3D linearized unsteady aerodynamic calculations conducted with LINFLUX[15–17] were used to gain significantly more insight regarding placement of the liner and choice of surface impedance. This analysis confirmed that a ρc-impedance was appropriate. It also indicated that, at least for this fan rig, the porous surface should be placed on the pressure side of the vane and should not extend beyond approximately 50% of the chord. The goal was to attenuate sound from 3000 to 9000 Hz.

Figure 5 provides sketches of two sets of chambers used in these soft vanes. These chambers were designed using the ILIAD code[8] mentioned earlier. A screenshot of the code is provided in Figure 6. The upper window shows the outline of the vane, with six possible chamber configurations formed to fit within the available volume. The window at the lower right provides real-time updates of the normal incidence acoustic impedance predicted for the treated surface, such that the user can monitor the impedance spectrum as the chamber geometry is altered. This approach allowed more detailed designs with a number of narrow chambers. Each chamber was designed to target a selected frequency and odd multiples of that frequency. The total number of chambers was split into two sets, and these sets of chambers were interleaved to form the final design. Additional samples were fabricated and tested in the NIT to confirm that the model was providing accurate predictions prior to fabrication of the final vanes for the SDT test.

(a) Set #1. (b) Set #2.

Figure 5: Sketch of two sets of chambers for SDT soft vane.

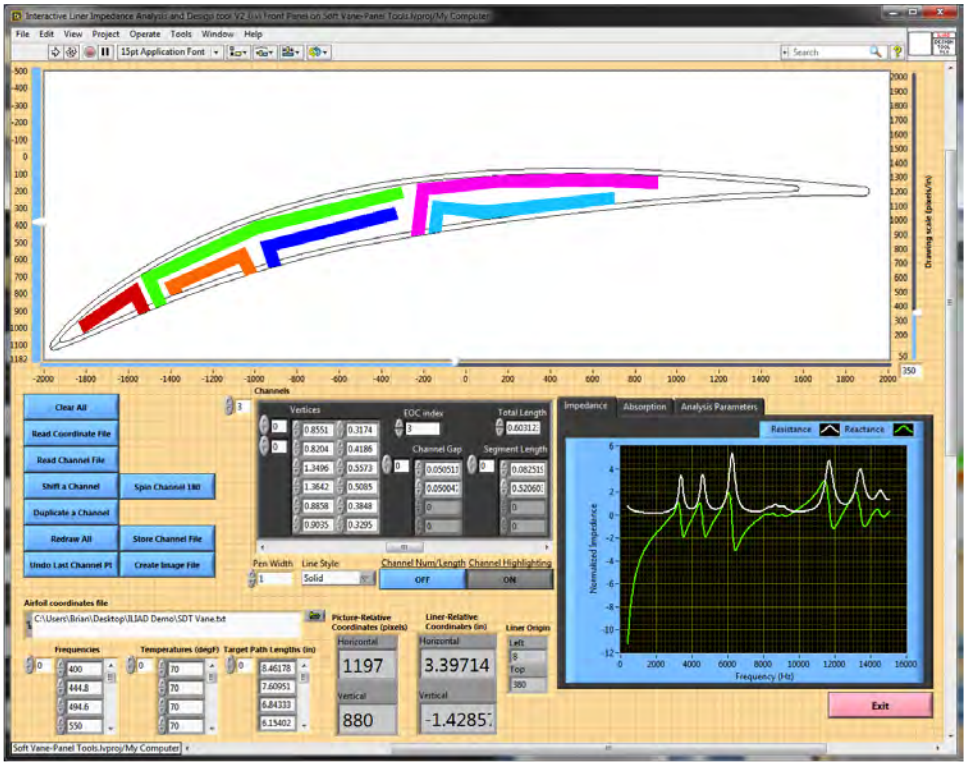

Figure 6: Screenshot of ILIAD code used for soft vane design.

Figure 7 provides photographs of an individual vane and of the full set of vanes as installed in the fan rig. Careful inspection of the individual vane confirms that there are two alternating patterns corresponding

to the two sets of chambers indicated in Figure 5. Test results from the SDT test indicate these soft vanes provided from 1 to as much as 3 dB attenuation over the full frequency range,[18] with an estimated 1.5 EPNdB (effective perceived noise level in decibels) noise reduction.

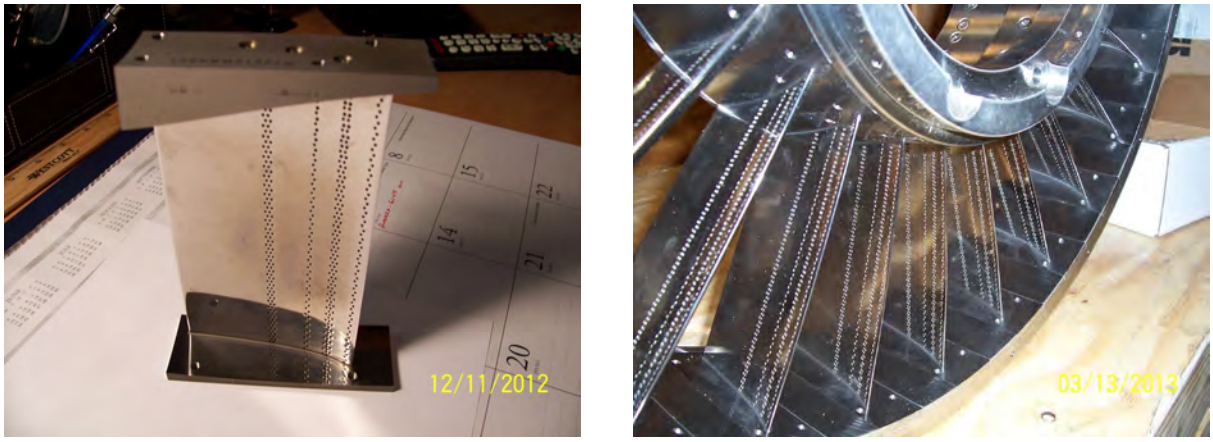

(a) Individual vane. (b) As installed.

Figure 7: Photographs of SDT soft vanes.

2. Key Points

There are a few points to be gleaned from these soft vane studies. First, the ability to use additive manufacturing to fabricate test articles suitable for testing in the NIT proved invaluable. The available volume for each of these vanes was quite limited, and the shape of the vane volume was quite different from that used for conventional acoustic liners mounted in the walls of the engine nacelle. This made the design process very challenging, e.g., ensuring that internal chambers had sufficient partition thickness to be effectively rigid as assumed in the impedance prediction model. LINFLUX calculations provided key guidance as to the optimum surface impedance and location of the treatment on the vanes. Also, ILIAD was instrumental for packaging arrays of resonators into the vanes, thereby allowing more complex configurations to be considered. Ideally, a three-dimensional version of ILIAD could be incorporated in future designs, such that the internal volume of the vanes could be more efficiently utilized. Finally, the ability to perform simple NIT tests with multiple configurations helped immensely in determining which configuration most closely matched the target impedance.

B. Over-the-Rotor Liner

1. Review

Over-the-rotor (OTR) liners were also evaluated in the same ANCF and LSWT tests.[2,3,14,19,20] Figure 8 provides photographs of one version of OTR liners, which employs metallic foam to achieve a desired impedance spectrum at the surface of the liner. Due to their location, OTR liners are expected to have the most significant effect on noise generated at the tips of the rotors. No analytical models were available to predict the optimum surface impedance for OTR liners. However, the sound is assumed to impinge on the fan containment case at normal incidence. Thus, for the same reasons as applied for the soft vane application, the target impedance for liners embedded in the fan containment case (i.e., OTR liners) was chosen to be ρc (normalized impedance of unity).

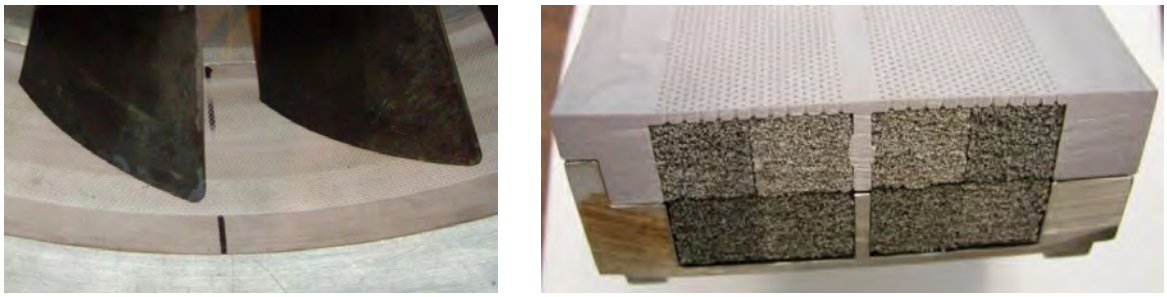

(a) Perforate rubstrip over metal foam.

(b) Edge view of metal foam installed beneath perforate.

Figure 8: Photographs of over-the-rotor metallic foam liner with perforate rubstrip.

This method of liner construction is based on two important properties. First, these metallic foams provide the required acoustic properties (porosity, density, tortuosity, etc.) to achieve the desired surface impedance spectrum. Second, these foams provide properties that support blade-out containment. They are not sufficient to fully achieve blade containment, but can be used to minimize requirements (i.e., reduce thickness and, thus, weight) for the fan containment case. OTR liners were evaluated both with and without a perforated facesheet covering the metallic foam.

Due to their construction, each of these configurations is an extended-reaction liner (i.e., sound can enter at one location on the surface and exit at a different location). However, as a result of excellent absorptive properties, the foams used in these tests behave as if they are local-reacting liners (see earlier discussion in Section II). As a result, the design and evaluation process was conducted using conventional methods typically used for local-reacting liners.

The process for design and evaluation of the metallic foam OTR liner concept was described in some detail in an earlier paper,[2] so the following discussion is limited to those items needed for the current discussion. Multiple types of metallic foam were considered for this study. These included Haynes 25 (cobalt alloy), FeCrAlY (composite foam consisting of iron, chromium, aluminum, and yttrium), and stainless steel. For each type of foam, NIT tests were conducted to determine the surface impedance of different thicknesses of foam, and the TTM was used to educe intrinsic acoustic properties (e.g., characteristic impedance and propagation constant) of the foam. Based on this information, the surface impedance of any (within reason) thickness of similar foam can be predicted.

The target frequency range for the ANCF tests was 1000 to 3000 Hz. Different foam densities and porosities (these were the parameters available from the manufacturer) were evaluated, first using the NIT for stand-alone foam tests and then for OTR liners mounted in the ANCF. Results indicated that the metallic foam with a density of 8% (consists of 8% metal and 92% air) and a porosity of 80 pores/inch provided the closest match to the desired impedance. Additional NIT tests also confirmed that similar results were achieved for all three types of metallic foam, i.e., the material is not important as long as it forms a rigid foam. When an 8% dense, 80 pores/inch, 2 in-thick, metallic foam liner (no facesheet) was placed in the ANCF, it was shown to provide 3 to 4 dB attenuation over approximately 2 octaves.

As mentioned earlier, the target frequency range for the ADP fan rig mounted in the LSWT was 1645 to 5306 Hz, i.e., the target impedance was unity over this frequency range. The 22 in fan rig provides a much higher mean flow over the surface of the liner. Thus, a perforated sheet was placed over the surface of the metallic foam (Fig. 8). Also, the depth of the metallic foam was limited to 1.5 in. Again, component tests were conducted in the NIT to select a final configuration based on the available resources (foam properties, thickness, perforated sheet). Unfortunately, there was a failure when this concept was tested in the LSWT.[20] During testing, there was significant air jetting in and out of the perforated sheet. This caused the metallic foam to erode, and also caused damage on the the surface of the rotating fan blades. It is not clear whether this was due solely to the increased impinging air flow, or if fragments of the metallic foam also impinged on the blade surface. Regardless, the test matrix for this concept had to be significantly reduced. Because of this, only limited acoustic benefits were demonstrated with this concept.

As mentioned earlier, a second test was conducted in the LSWT with the SDT fan rig, with a goal of

noise reduction over the frequency range of 3000 to 9000 Hz. Because of the issues experienced with the metallic foam in the earlier test, OTR liners were designed that employed multiple, variable-depth, resonant chambers (Fig. 9). A number of configurations were considered, in which the number of chambers and depth of those chambers were varied. Figure 10 provides two photographs of one of the configurations tested in the NIT. These chambers were designed as slots with rounded edges to simplify the fabrication process and to allow a number of chambers to be squeezed into a tight volume. A grooved cover sheet was placed over the surface for the LSWT test. This was designed for aerodynamic purposes, but the effects of the grooves were also considered in the acoustic predictions.

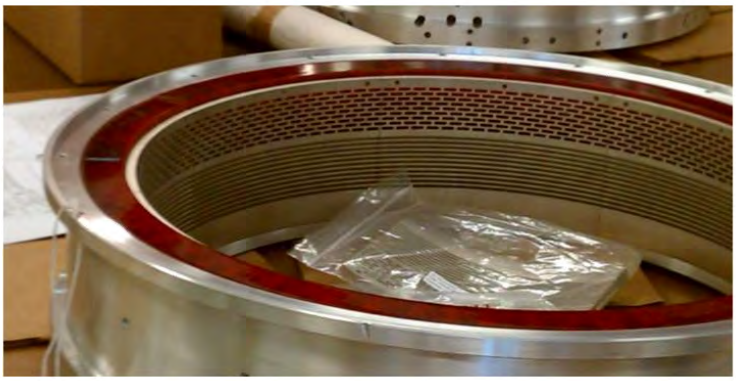

Figure 9: Photograph of over-the-rotor resonant-chamber liner used in SDT test.

The results achieved with the SDT fan rig were mixed. It was determined that the grooved cover sheet generated additional broadband noise, only some of which was attenuated by the OTR liner. Thus, much more detailed analysis is needed to extract benefits due to the variable-depth liner. Regardless, it is clear that a future design of OTR liners would require adjustments to the design of the cover sheet and would likely employ resonant chambers.

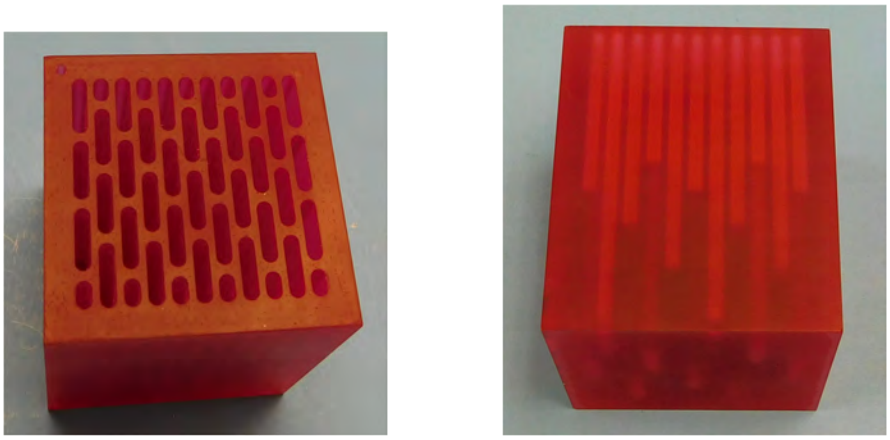

(a) Top view. (b) Side view.

Figure 10: Photographs of OTR sample tested in NIT.

2. Key Points

The metallic foams considered for this application provided excellent acoustic and containment properties, and they provided very good results in component tests with the NIT and low TRL (technology readiness level) tests in the ANCF. However, tests with this concept had to be aborted in the 22 in fan rig due to problems with increased air jetting and/or metal foam impingement onto the blade surface. As a side note, an additional metallic foam OTR liner was evaluated in an FJ44 turbofan engine,[19] and was shown to provide approximately 5 dB over a significant frequency range. A follow-on test employed variable-depth, resonant chambers, and met with limited success. The successful results of the lower TRL tests (and the FJ44 engine test) suggest that the initial choice of surface impedance was appropriate for this application, but analytical tools are needed to more thoroughly explore this hypothesis. Again, the ability to use NIT tests for evaluation of different configurations was very helpful.

C. External Liner

1. Review

The third novel concept is the external liner. Figure 11 provides a photograph of external liners mounted on a hybrid wing body (HWB) airframe for tests in the Boeing Low Speed Aeroacoustic Facility (LSAF) as part of a NASA/Boeing collaboration.[21,22] An open rotor fan rig with two counter-rotating rows of blades is mounted above an HWB airframe in the LSAF, and acoustic liners are mounted on the external surface of the HWB to reduce the amount of sound reflected to the far field. A wing liner is mounted below the open rotor fan, and two elevon liners are mounted at the trailing edge of the airframe. This test model is constructed in a modular fashion, such that different liner configurations can be installed in the surface of the elevons and the wing. The optimum impedance for each of these locations was not known when the liners were being designed, so a ρc surface impedance was again chosen as the goal.

Multiple configurations were considered for each liner type (wing and elevon liners). Some of these configurations (Figs. 12 and 13) incorporated variable-depth, resonant chambers that communicate with the surface via a perforated facesheet. The ILIAD code was used for these designs, such that use of the available volume could be optimized. However, these designs were confined to 2-D configurations. In other words, all chambers with surfaces along a single chord line were confined in the spanwise dimension such that none of them intersected with the neighboring chambers in the adjacent row of chambers. These variable-depth liners were constructed via additive manufacturing. Extended-reaction configurations were also tested, in which the liner consisted of a wire frame filled with a bulk material.

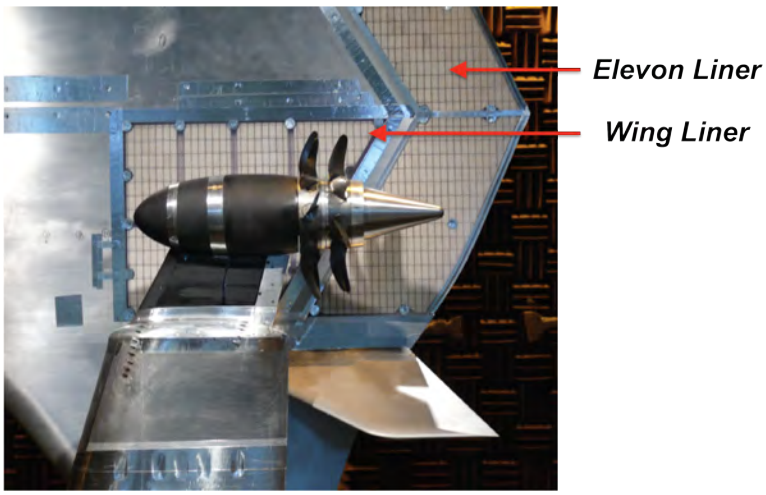

Figure 11: Photograph of external (elevon and wing) liners mounted in Boeing Low Speed Aeroacoustic Facility. (Photo provided by The Boeing Company)

2. Wing Liners

Three wing liner configurations were designed and tested. The goal for the first (Fig. 12a) was to absorb sound over the full frequency range of interest, 2040 to 6120 Hz. The total depth of this liner, including an 0.25 in-thick solid backplate, was 1.25 in. A single liner block consisted of five bent ('L'-shaped) chambers with total depths (combination of individual segments) of 1.3 to 2.9 in, and extended over an axial length of 2.2 in. These chamber depths correspond to the quarter-wavelengths for frequencies of 1150 to 2600 Hz. However, resonant chambers also provide absorption at odd multiples of the resonant frequency (corresponding to $^3/_4\lambda$, $^5/_4\lambda$, etc.). When these effects are included, absorption can occur over a wider frequency range. This 5-chamber pattern was repeated over the full length of the liner.

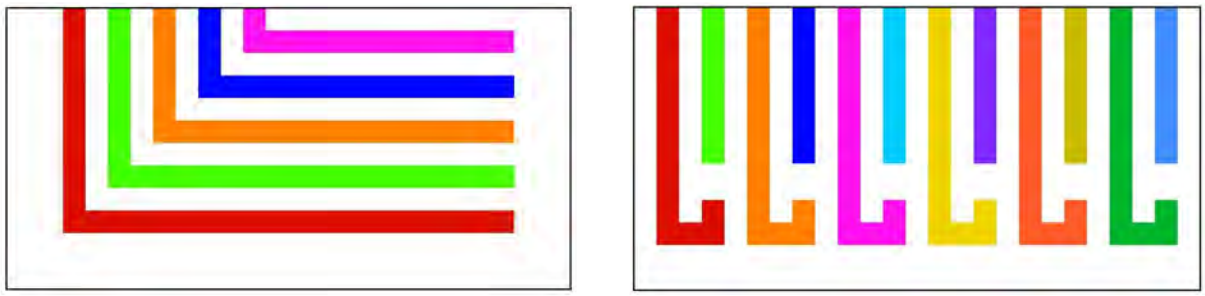

(a) Single (repeated) block of wing liner - version 1.

(b) Single (repeated) block of wing liner - version 2.

Figure 12: Sketches of variable-depth, resonant-chamber, wing liners. Upper (flow) surface is porous for both liners.

The second wing liner targeted BPF and 2BPF at takeoff (2400 and 4800 Hz), respectively. This configuration, shown in Fig. 12b, consisted of two unique chambers with depths of 1.35 and 0.69 in, again with a total liner depth of 1.25 in. The longer of these chambers was designed as a 'J' chamber such that it would fit within the available space, while the other was a straight chamber. As with the first configuration, these two chambers were repeated over the full length of the wing liner.

The third configuration used Nomex^{TM}foam embedded within a wire frame (Fig. 11) to achieve a near-ρc surface impedance. Various types of foam were evaluated using the TTM with data acquired in the NIT, from which a 0.5 in-thick layer of foam with a density of 5.7 lb/ft^3 was chosen. This configuration was shown to provide a normalized acoustic resistance (real component of impedance) very near unity. Although this is an extended-reacting liner, it was expected to behave similar to a local-reacting liner with the same surface impedance since the material provides significant absorption (see earlier discussion).

3. Elevon Liners

Three configurations were also considered for the elevon liners. The tapering liner thickness (1 in at LE, 0.125 in at TE) introduced an additional design constraint. Given the limited volume in the aft portion of the elevon, this meant the target impedance could not be uniformly maintained over the entire surface of the liner without taking extraordinary measures. Since there was no specific guidance as to the optimum impedance, this was not done.

The goal of the first two elevon liners (Fig. 13) was to achieve sound absorption over the full frequency range of interest (2040 to 6120 Hz) by employing variable-depth chambers. One employed bent chambers, while the other was constrained to only use straight chambers. The first configuration employed chambers ranging in depth from 1.73 in at the LE to 0.09 in at the TE. The longest of these was tuned to the lower frequency limit (approximately 2000 Hz), and the shortest was tuned to well beyond the upper limit (>35 kHz). This high frequency tuning was driven by the limited TE thickness of the elevon. Rather than incorporate a few longer chambers near the TE, with dead space in between, the chosen design provided a uniform distribution of porosity at the liner surface. The second configuration employed variable-depth,

straight chambers that varied linearly from a maximum depth of 0.89 in at the liner LE to a minimum depth of 0.11 in at the TE to target the full frequency range.

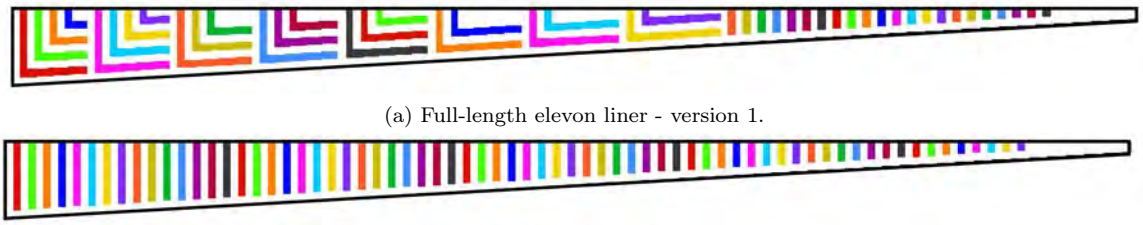

(a) Full-length elevon liner - version 1.

(b) Full-length elevon liner - version 2.

Figure 13: Sketches of variable-depth, resonant-chamber, elevon liners. Upper (flow) surface is porous for both liners.

Each of these variable-depth liners provides an impedance that varies over the surface of the liner. This is quite different from the uniform, ρc surface impedance that was desired. Instead, this approach targets each frequency in a sequential fashion. The chambers near the LE (where the liner is thicker) target a ρc surface impedance for the lower frequencies and the chambers near the TE (thinner region) target the same impedance for higher frequencies. Essentially, this design process assumes that each chamber operates solely for the frequency for which it is tuned, and that there is no interaction between adjacent chambers. This is clearly not the case. Nevertheless, since the optimum impedance was not known, there was no *a priori* reason to believe that this design would be worse (or better) than a uniform ρc impedance.

The last elevon liner used Nomex^{TM}foam embedded within a wire frame (Fig. 11), the same as was used in the wing liner (above). Although the tapering geometry reduces the foam thickness near the TE, this configuration provides a more uniform impedance over the liner surface than was achieved with the variable-depth configuration.

4. Key Points

As indicated in earlier reports,[21,22] the wing and elevon liners that consisted of a wire frame with embedded foam provided the best results. The sound field of an open rotor that is shielded by an airframe results in a very complex distribution of sound in the far field. While there were reductions of up to 8 dB over large angular ranges, there were also increases in the levels at other angles. Perhaps a better assessment of these external liners is provided on a system noise level. As indicated by Thomas et al.,[22] an 0.7 EPNdB cumulative benefit (Effective Perceived Noise Level, sum of values at approach, cutback and takeoff) was achieved with external liners that employed Nomex^{TM}foam. The resonant-chamber liners also provided attenuation over the desired frequency range, but not as much as was achieved with the foam liners shown in Figure 11. Given the assumptions that were applied in the liner design process, these results were very promising.

It is important to note that these liners extended over the full portion of available surface. Ideally, the extent of these liners would be reduced in a future design. Since these liners are, by definition, on the outer surface of the aircraft, there are concerns regarding additional drag due to the roughness at the liner surface. Separate studies[23,24] are being conducted by the Langley Liner Physics Team to develop low-drag concepts that would alleviate (or at least minimize) this concern. Nevertheless, a reduction in the surface area would be desired.

Prediction codes exist to explore the three-dimensional scattered acoustic field due to sound interacting with an airframe surface, whether or not that surface contains an acoustic liner.[25] However, realistic source predictions for the open rotor were not readily available at the time of these tests (2009 - 2011), which meant these codes could not be used to guide the design process. This issue has since been alleviated.[26] Thus, a new design would allow external liners to be placed only at the most beneficial locations. Also, this type of analysis would provide a true target impedance for these liners. Given the success achieved with the initial

tests, for which there was very limited design information, this area of research is clearly worthy of further investigation.

D. Flap Side-Edge Liner

1. *Review*

The last concept to be discussed is the flap side-edge liner.[27] Flap noise is caused by the generation of a vortex near the corner of the flap that rolls up over the surface of the flap. A liner embedded in the body of the flap side edge absorbs some of the noise that is generated by this process. It also provides a pressure-release surface, thereby weakening this vortex generation process. Each of these processes contributes to a reduction in flap noise.

In 2013, an 18% scale, semi-span, high-fidelity replica of a Gulfstream aircraft was tested in the NASA Langley 14- by 22-Foot Subsonic Tunnel. A number of flap side-edge liner configurations were evaluated for their potential to reduce airframe noise produced at the edges of flaps. This test is discussed in some detail by Khorrami,[28] so the following will be limited to those items that are pertinent to the current study. Since the main test was on an 18% scale model, the target range for this study was 600 to 35,000 Hz. Based on prior studies,[29,30] the target normalized resistance was projected to be between 1.0 and 1.9, and the target normalized reactance was zero. As depicted in Figure 14, tests were conducted with flap side-edge liners incorporated into the inboard and outboard flap edges.

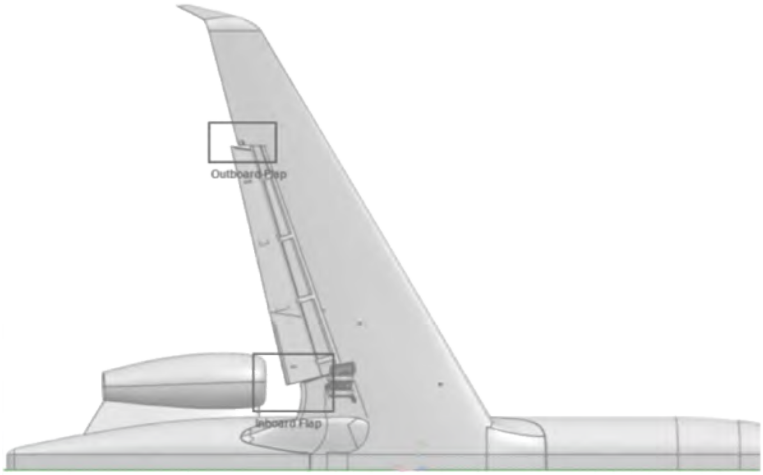

Figure 14: Artist's sketch depicting locations of inboard and outboard flaps.

Three types of flap side-edge liner were considered. The first employed a large array of variable-depth, serpentine chambers (see Fig. 15a). Given the limited volume, the design approach was to tune the chamber depths to quarter-wavelengths corresponding to frequencies from 600 to 10,000 Hz. The expectation was that the odd multiples of these frequencies (corresponding to $3/4\lambda$, $5/4\lambda$, etc.) would fill in the remainder of the desired frequency range. Given the small size of the portion of the flap used for the liner, together with the desired chamber depths, a 3-dimensional design approach was used, i.e., many of the chambers were intertwined within the volume of the flap. This meant the the ILIAD code could not be used for this study. The impedance prediction model was used to determine the appropriate combination of chamber depths, and the design process to embed the chambers within the available space was done by hand, an extremely tedious and painstaking process! Also, the interior volume near the tips was not sufficient to house an appropriate number of chambers, which meant the target impedance could not be achieved uniformly over the entire surface.

The second type of flap side-edge liner consisted of an empty cage-like structure covered with wire mesh (see Fig. 15b). The wire mesh was used to smooth the surface and to provide a resistance drop. Four

meshes were considered, with DC flow resistances of 150, 270, 450, and 570 MKS Rayls (normalized DC flow resistances of 0.36, 0.65, 1.10, and 1.37).

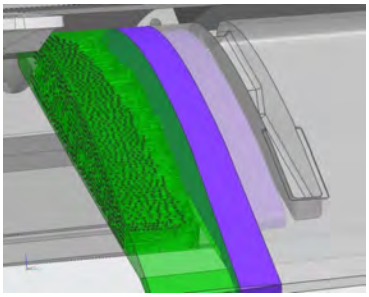

(a) Serpentine chamber liner.

(b) Wire cage with mesh cover sheet.

Figure 15: Depictions of flap side-edge liner.

The third liner type employed the same cage-like structure. A low-resistance (20 MKS Rayls) wire mesh was used for this configuration, and the interior was filled with foam to achieve the desired surface impedance. Three types of foam were considered - Nomex^{TM}and two types of FeCrAlY. The TTM was used to evaluate each of these materials based on NIT measurements for multiple thicknesses. Based on these results, it was determined that each of the three types of foam, when covered with the wire mesh, provided a resistance within the desired range. Also, each foam provided sufficient absorption to subdue the extended-reaction properties, such that these liners were assumed to behave as local-reacting liners.

2. Key Points

Each flap side-edge liner provided noise reduction in the 14- by 22-Foot Subsonic Tunnel test. The best results were achieved with the bulk liners (low-resistance wire mesh with embedded foam). Sound pressure level reductions of 2 to 4 dB over the entire frequency range at all directivity angles were observed.[28] Given the minimal amount of treatment required for this application, this concept certainly warrants further study.

As briefly discussed above, the ILIAD code could not be used to design the variable-depth, flap side-edge liner because the chambers had to be intertwined to fit within the available volume. This portion of the design process therefore had to be completed by hand. This points to a clear need for a three-dimensional version of the ILIAD that would allow these complex chamber shapes to be incorporated in a user-friendly manner. This is the subject of a current investigation.

IV. Concluding Remarks

This paper has presented a brief review of four novel liner concepts: soft vanes, over-the-rotor liners, external liners, and flap side-edge liners. While these concepts are quite disparate, they share a number of design features. Also, since the tests described herein represented the first investigations of these concepts, there was typically limited information to guide the design process. The target frequencies (or range of frequencies) were known, but the optimum impedance was only known for the flap side-edge liners.

Soft vane tests were conducted in the NASA Glenn 9- by 15-Foot Low Speed Wind Tunnel with two 22 in-diameter fan rigs. They provided 1 to 2 dB attenuation over at least two octaves when mounted in the Advanced Ducted Propulsor fan rig, and 1 to 3 dB attenuation over the full frequency range (system level benefit of 1.5 EPNdB) when mounted in the Source Diagnostic Test fan rig. Over-the-rotor liners provided 3 to 4 dB attenuation over two octave bands in the NASA Glenn Advanced Noise Control Fan. Follow-on tests with the Advanced Ducted Propulsor fan rig had to be limited due to significant air jetting (and possibly metallic foam) impingement on the surface of the fan blades. A resonant-chamber configuration was used in the Source Diagnostic Test fan rig test. The results from this test indicate the liner provided attenuation. However, it appears the grooved design of the facesheet introduced self-noise that inhibited the

liner performance. External liners (wing liner plus two elevon liners) provided 0.7 EPNdB reduction of noise generated by an open rotor engine mounted above a hybrid wing body airframe in the Boeing Low Speed Aeroacoustic Facility. Finally, flap side-edge liners mounted on a semi-span model of a Gulfstream aircraft in the NASA Langley 14- by 22-Foot Wind Tunnel provided 2 to 4 dB attenuation over the full range of interest.

The suite of tools mentioned earlier was critical for design and evaluation of each of these concepts, first at the component level (i.e., NIT tests) and then for the full tests in the larger facilities. The impedance prediction model was used to design variable-depth configurations for each concept. The ILIAD code was developed to support this design process, and proved extremely beneficial for the soft vane and external liner applications. However, the current two-dimensional limitation of ILIAD meant it could not be used to design the variable-depth, serpentine chamber, flap side-edge liner. Instead, this process was completed by hand. Since the completion of this study, work has begun on a three-dimensional version of the code that will support complex chamber geometries.

This set of tests has extended over the last decade. During that period of time, significant advances have occurred in additive manufacturing. As a result, significantly more complex configurations can now be considered. This development is important not only for the final liners to be used in the large-scale tests, but also for component tests conducted using the normal incidence tube. The ability to quickly fabricate and test different configurations is quite valuable. Simple normal incidence tube tests of bulk materials were also quite helpful in the down-select process. The Two-Thickness Method was used extensively in this process.

One significant concern is the lack of sufficient information to guide the design process. Specifically, the liner designer needs to be provided with the target impedance and the optimum location where that impedance should be achieved at the surface of each type of liner. For the majority of these tests, the target impedance was not known. For these cases, a ρc-impedance was chosen as the target, based on the expectation that the sound field (for these three applications) impinges on the surface of the liner at normal incidence. Since these tests were completed, further modeling and code development has occurred, which offers promise for providing this much needed information. Regardless, the results achieved with these liners are very encouraging.

Acknowledgments

The Advanced Air Transport Technology Project of NASA's Advanced Air Vehicles Program funded this work. The support of Carol Harrison of the NASA Langley Structural Acoustics Branch for normal incidence tube testing of numerous liner configurations is gratefully acknowledged. Contributions from Dave Elliott, Ed Envia, Chris Hughes, Chris Miller, and Dan Sutliff of the NASA Glenn Acoustics Branch, as well as Dan Tweedt of AP Solutions, Inc., and Jim Buckley of Vantage Partners, are gratefully acknowledged with regard to the soft vane and over-the-rotor liner investigations. Contributions of Russ Thomas of the NASA Langley Aeroacoustics Branch and Michael Czech of the Boeing Company are gratefully acknowledged with regard to the external liner investigation. Finally, contributions of Meelan Choudhari, Mehdi Khorrami, and Dave Lockard of the NASA Langley AeroSciences Branch are gratefully acknowledged with regard to the flap side-edge liner investigation.

References

[1]Jones, M. G., Parrott, T. L., Heidelberg, L. J., and Envia, E., "Low-Noise Fan Exit Guide Vanes," U.S. Patent 7334998, February 2008.

[2]Jones, M. G., Parrott, T. L., Sutliff, D. L., and Hughes, C. E., "Assessment of Soft Vane and Metal Foam Engine Noise Reduction Concepts," AIAA Paper 2009-3142, May 2009.

[3]Sutliff, D. L. and Jones, M. G., "Foam-Metal Liner Attenuation of Low-Speed Fan Noise," AIAA Paper 2008-2897, May 2008.

[4]Sutliff, D. L., Elliott, D. M., Jones, M. G., and Hartley, T. C., "Attenuation of FJ44 Turbofan Engine Noise with a Foam-Metal Liner Installed Over-the-Rotor," AIAA Paper 2009-3141, May 2009.

[5]Parrott, T. L. and Jones, M. G., "Parallel-Element Liner Impedances for Improved Absorption of Broadband Sound in Ducts," *Noise Control Engineering Journal*, Vol. 43, No. 6, November - December, 1995.

[6]Motsinger, R. E. and Kraft, R. E., "Design and Performance of Duct Acoustic Treatment: Aeroacoustics of Flight Vehicles; Chapter 14, Vol. 2: Noise Control," NASA RP 1258, August 1991.

[7]Jones, M. G., Howerton, B. M., and Ayle, E., "Evaluation of Parallel-Element, Variable-Impedance, Broadband Acoustic Liner Concepts," AIAA Paper 2012-2194, June 2012.

[8]Howerton, B. M., Jones, M. G., and Buckley, J. L., "Development and Validation of an Interactive Liner Design and Impedance Modeling Tool," AIAA Paper 2012-2197, June 2012.

[9]Howerton, B. and Jones, M., "A Graphical Acoustic Liner Design and Analysis Tool," Patent Pending.

[10]Jones, M. G., Parrott, T. L., and Watson, W. R., "Uncertainty and Sensitivity Analyses of a Two-Parameter Impedance Prediction Model," AIAA Paper 2008-2928, May 2008.

[11]Chung, J. Y. and Blaser, D. A., "Transfer function method of measuring in-duct acoustic properties: I. Theory," *Journal of Acoustical Society of America*, Vol. 68, 1980, pp. 907–921.

[12]Jones, M. G. and Parrott, T. L., "Evaluation of a multi-point method for determining acoustic impedance," *Journal of Mechanical Systems and Signal Processing*, Vol. 3, No. 1, 1989, pp. 15–35.

[13]Smith, C. D. and Parrott, T. L., "Comparison Of Three Methods For Measuring Acoustic Properties Of Bulk Materials," *Journal of Acoustical Society of America*, Vol. 74, No. 5, 1983, pp. 1577–1582.

[14]Hughes, C. E. and Gazzaniga, J. A., "Effect of Two Advanced Noise Reduction Technologies on the Aerodynamic Performance of an Ultra High Bypass Ratio Fan," AIAA Paper 2009-3139, May 2009.

[15]Montgomery, M. D. and Verdon, J. M., "A Three-Dimensional Linearized Unsteady Euler Analysis for Turbomachinery Blade Rows," NASA CR 4770, 1997.

[16]Chuang, H. A. and Verdon, J. M., "A Numerical Simulator for Three-Dimensional Flows Through Vibrating Blade Rows," NASA CR 1998-208511, 1998.

[17]Verdon, J. M., "Linearized Unsteady Aerodynamic Analysis of the Acoustic Response to Wake/Blade-Row Interaction," NASA CR 2001-210713, 2001.

[18]Elliott, D. M., "Over the Rotor and Soft Vanes on the Source Diagnostic Test Model in the NASA Glenn 9x15 Low Speed Wind Tunnel," to be published as a NASA TM.

[19]Sutliff, D. L. and Jones, M. G., "Low-Speed Fan Noise Attenuation from a Foam-Metal Liner," *Journal of Aircraft*, Vol. 46, No. 4, July 2009, pp. 1381–1394.

[20]Elliott, "Acoustic Performance of Unique Liner Locations for a High Bypass Model Turbofan at Simulated Flight Conditions," AIAA Paper 2009-3140, May 2009.

[21]Czech, M. J. and Thomas, R. H., "Open Rotor Aeroacoustic Installation Effects for Conventional and Unconventional Airframes," AIAA Paper 2013-2185, 2013.

[22]Thomas, R. H., Burley, C. L., Lopes, L. V., Bahr, C. J., Gern, F. H., and Zante, D. E. V., "System Noise Assessment and the Potential for a Low Noise Hybrid Wing Body Aircraft with Open Rotor Propulsion," AIAA Paper 2014-0258, January 2014.

[23]Howerton, B. M. and Jones, M. G., "Acoustic Liner Drag: A Parametric Study of Conventional Configurations," AIAA Paper 2015-2230, June 2015.

[24]Gerhold, C. H., Brown, M. C., and Jasinski, C. M., "Evaluation of Skin Friction Drag for Liner Applications in Aircraft," AIAA Paper 2016-1267, January 2016.

[25]Tinetti, A. F. and Dunn, M. H., "Aeroacoustic Noise Prediction Using the Fast Scattering Code," AIAA Paper 2005-3061, May 2005.

[26]Nark, D. M., Jones, W. T., D. D. Boyd, J., and Zawodny, N. S., "Isolated Open Rotor Noise Prediction Assessment Using the F31A31 Historical Blade Set," AIAA Paper 2016-1271, January 2016.

[27]Jones, M., Khorrami, M., Choudhari, M., and Howerton, B., "Flap Side Edge Liners for Airframe Noise Reduction," U.S. Patent 8695915, April 2014.

[28]Khorrami, M. R., W. M. Humphreys, J., Lockard, D. P., and Ravetta, P. A., "Aeroacoustic Evaluation of Flap and Landing Gear Noise Reduction Concepts," AIAA Paper 2014-2478, June 2014.

[29]Choudhari, M. and Khorrami, M. R., "Computational Study of Porous Treatment for Altering Flap Side Edge Flow Field," AIAA Paper 2003-3113, May 2003.

[30]Horne, W. C., James, K. D., Arledge, T. K., Soderman, P. T., Burnside, N., and Jaeger, S. M., "Measurements of 26%-Scale 777 Airframe Noise in the NASA Ames 40- by 80-Foot Wind Tunnel," AIAA Paper 2005-2810, May 2005.